

(C 204730)
030619

TOMOGRAPHIC IMAGING OF THE SUN'S INTERIOR

A. G. KOSOVICHEV

W. W. Hansen Experimental Physics Laboratory, Stanford University, Stanford, CA 94305-4085

Received 1996 January 11; accepted 1996 January 26

ABSTRACT

A new method is presented of determining the three-dimensional sound-speed structure and flow velocities in the solar convection zone by inversion of the acoustic travel-time data recently obtained by Duvall and coworkers. The initial inversion results reveal large-scale subsurface structures and flows related to the active regions, and are important for understanding the physics of solar activity and large-scale convection. The results provide evidence of a zonal structure below the surface in the low-latitude area of the magnetic activity. Strong converging downflows, up to 1.2 km s^{-1} , and a substantial excess of the sound speed are found beneath growing active regions. In a decaying active region, there is evidence for the lower than average sound speed and for upwelling of plasma.

Subject headings: convection — methods: data analysis — Sun: activity — Sun: oscillations — sunspots

1. INTRODUCTION

Sound waves excited in the subsurface granulation layer propagate into the Sun's interior along ray paths which are refracted toward the surface because the speed of sound increases with the depth. When the sound speed becomes sufficiently high the waves are reflected and return to the surface at some distance from their origin. The travel time of the waves depends primarily on the speed of sound (wave group velocity, more precisely) and on the velocity of flow along the ray paths. The effects of the sound-speed structure and of flows can be separated by measuring the travel time of waves propagating in opposite directions along the same ray paths. Duvall et al. (1993) have discovered that the travel time can be measured for groups of rays despite the stochastic nature of solar sound and turbulent noise on the surface. Such measurements provide a means for probing the three-dimensional structures of the internal sound speed and flows.

Recently, Duvall et al. (1996) have published maps of the travel times of sound waves propagating in local regions in the convection zone. The maps represent measurements of the time for acoustic waves to travel between points on the solar surface and surrounding annuli. The measurements were obtained by estimating cross-correlation functions of fluctuations of brightness of the solar surface, caused by 5 minute acoustic oscillations. The waves are stochastically excited by granulation uniformly distributed on the surface; therefore, there are waves propagating between any two points on the surface. However, because of the high level of noise, the data are averaged over large surface areas. Typically, the measurements represent a mean travel time between a central point and surrounding annuli, which were chosen in four radial distance ranges, Δ : 2.5–4.25, 4.5–7, 7.25–10, and 10.25–15 heliographic degrees ($1^\circ \approx 12.15 \text{ Mm}$). The acoustic rays that propagate to these radial distances span the upper 30% of the convection zone, penetrating to a depth, z , of about 64 Mm (Fig. 1).

Two sets of data were obtained during 17 hr of continuous observations at the South Pole in 1991. The first represents the mean of the travel time τ^+ for the rays propagating from a central point to the surrounding annuli and the time τ^- for the rays propagating in the opposite direction. The second set is

the difference of these travel times. The mean travel time, $0.5(\tau^+ + \tau^-)$, depends primarily on the sound speed along the ray paths, while the difference $\tau^+ - \tau^-$ is sensitive to the flow velocity. The observed area is shown in Figure 2 (Plate L8). The spatial resolution of the data is 1.75° (21.3 Mm) in both longitude and latitude.

We have developed an inversion method to infer the structure of the sound speed and flow velocities from the data. The technique is somewhat similar to seismic tomography (e.g., Howe, Worcester, & Spindel 1987; Iyer & Hirahara 1993); however, it is more complicated computationally because each data point is no longer a one-dimensional line integral but is an average over $\sim 10^3$ ray paths that sample a large three-dimensional region (Fig. 1).

2. THE INVERSION METHOD

The travel time, τ_i , along a single ray path, Γ_i , in the geometrical optics approximation can be expressed in terms of the sound speed (wave group velocity), $c(\mathbf{x}, t)$, and the flow velocity $\mathbf{v}(\mathbf{x}, t)$:

$$\tau_i(t) = \int_{\Gamma_i} \frac{ds}{c(\mathbf{x}, t) + \mathbf{v}(\mathbf{x}, t) \cdot \mathbf{n}}, \quad (1)$$

where \mathbf{x} is the spatial coordinate, t is the time, s is the distance along the ray, and \mathbf{n} is a unit vector tangent to the ray. The sign of $\mathbf{v} \cdot \mathbf{n}$ depends on the direction of propagation; therefore, the travel time in opposite directions differs due to the effects of flows. Since variations of the travel time in the area of observation do not exceed 5%, the effects of flow and sound-speed inhomogeneity can be considered, in the first approximation, as perturbations to a horizontally uniform static reference model with a sound speed $c_0(\mathbf{x})$. Then the reference travel time is $\tau_{0,i} = \int_{\Gamma_{0,i}} ds/c_0(\mathbf{x})$.

Fermat's principle applied to the variation of the travel time gives

$$\delta\tau_i(t) \equiv \tau_i(t) - \tau_{0,i} = - \int_{\Gamma_{0,i}} \frac{\delta c(\mathbf{x}, t) \pm \mathbf{v}(\mathbf{x}, t) \cdot \mathbf{n}}{c_0^2(\mathbf{x})} ds, \quad (2)$$

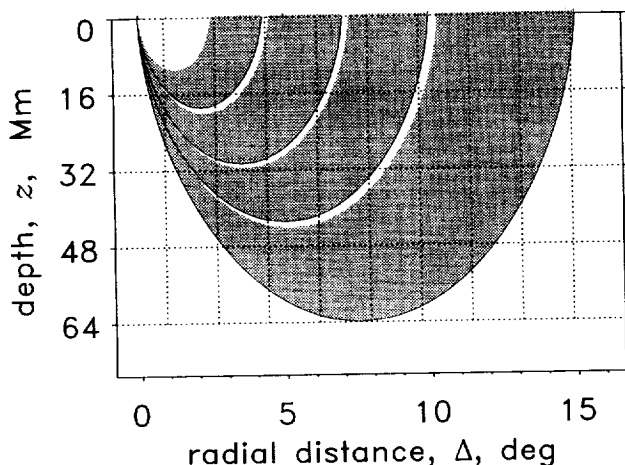


FIG. 1.—Regions of ray propagation (shaded areas) corresponding to the measurements by Duvall et al. (1996), as a function of depth, z , and the radial distance, Δ , from a point on the surface. The rays are also averaged over circular regions on the surface, forming three-dimensional figures of revolution. The dashed lines are the boundaries of the cells of the inversion model.

where the plus sign is for the rays propagating from the central point, $\Delta = 0$, to the annuli, and the minus sign is for the rays propagating in the opposite direction. The average and the difference between the travel time residuals are

$$\delta\tau_i^{\text{aver}}(t) \equiv \frac{1}{2} [\delta\tau_i^+(t) + \delta\tau_i^-(t)] = - \int_{\Gamma_{0,i}} \frac{\delta c(\mathbf{x}, t)}{c_0^2(\mathbf{x})} ds, \quad (3)$$

$$\delta\tau_i^{\text{diff}}(t) \equiv \delta\tau_i^+(t) - \delta\tau_i^-(t) = -2 \int_{\Gamma_{0,i}} \frac{\mathbf{v}(\mathbf{x}, t) \cdot \mathbf{n}}{c_0^2(\mathbf{x})} ds. \quad (4)$$

We assume that δc and \mathbf{v} did not change during the observations and represent them by a discrete model. In the model, the three-dimensional region of wave propagation is divided into rectangular blocks. We also assume that the relative perturbations of the sound speed, $\delta c/c$, and the ratio of the flow velocity to the sound speed, $\mathbf{M} \equiv \mathbf{v}/c$, are constant within the blocks. Then

$$\delta \ln c(\mathbf{x}, t) = \delta \ln c_{ijk}, \quad \mathbf{M}(\mathbf{x}, t) = \mathbf{M}_{ijk}, \quad (5)$$

where δc_{ijk} and \mathbf{M}_{ijk} are the unknown parameters of a block of the spatial coordinate indices i, j , and k .

According to Duvall et al.'s (1996) averaging procedure, the travel time measured at a point on the surface is the result of the cumulative effects of the perturbations in each of the traversed rays of the three-dimensional ray systems (Fig. 1). Therefore, we average equations (3) and (4) over the ray systems corresponding to the four radial distance intervals of the data, using approximately the same number of ray paths as in the observational procedure. As a result, we obtain two systems of linear equations that relate the data to the sound-speed variation and to the flow velocity:

$$\delta\tau_{\lambda\mu\nu}^{\text{aver}} = \sum_{ijk} A_{ijk}^{\lambda\mu\nu} \delta \ln c_{ijk}, \quad (6)$$

$$\delta\tau_{\lambda\mu\nu}^{\text{diff}} = \sum_{ijk, \alpha} B_{ijk, \alpha}^{\lambda\mu\nu} M_{ijk, \alpha}, \quad (7)$$

where λ and μ label the central points ($\Delta = 0$) of the ray systems in the observed area; ν (1, ..., 4) labels the radial

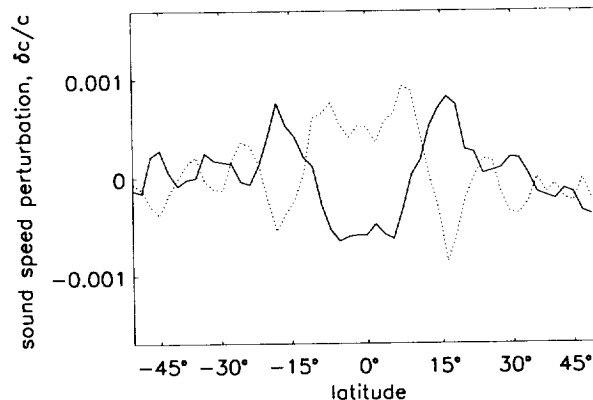


FIG. 4.—Azimuthally averaged perturbation of the sound speed as a function of latitude in the upper layer, 0–16 Mm (solid curve), and in the second layer, 16–32 Mm (dotted curve).

distance ranges (or annuli); i, j, k are the indices of the rectangular blocks of the three-dimensional structure model; and α denotes three components of the flow velocity. Equations (6) and (7) have been solved by a regularized least-squares technique (Paige & Saunders 1982). The mathematical details of the inversion procedure and tests will be published elsewhere.

3. THE INVERSION RESULTS

The travel-time anomalies have been measured by Duvall et al. (1996) for four sets of rays propagating from each of 72×52 points to the surrounding annuli (Fig. 1). The points are equally spaced in the observed area of $123^\circ \times 106^\circ$ on the solar surface (Fig. 2). For inversion of the data, we have adopted a four-layer discrete model. The layers which all are 16 Mm thick have been divided into 72×52 rectangular blocks of approximately the same size as the spacing between the data points.

The results of inversion are shown in Figure 2 and in Figure 3 (Plate L9) as maps of the sound-speed perturbation, $\delta c/c$, and the three components of the flow velocity, \mathbf{v} , in the four layers of our discrete model. They can be compared with the Ca^+ K-line intensity map in Figure 2. Perhaps the most interesting detail on the sound-speed map is the equatorial belt of the lower sound speed in the upper layer and higher speed in the lower layers. The belt is surrounded by narrow regions of the higher sound speed at latitude $\approx \pm 15^\circ$. This could be evidence of a thermal shadow due to a band of magnetic field in the convection zone. The thermal shadow was suggested by Parker (1987), who argued that the broad bands of azimuthal field in the convection zone should produce cool shadows which press the field downward, and force it to remain in the lower convection zone, balancing the magnetic buoyancy. Evidence for the thermal shadow has been previously reported by Kuhn, Libbrecht, & Dicke (1988) from photometry observations of the surface brightness, and by Goode & Kuhn (1990) from splitting of p -mode frequencies. Figure 4 shows latitudinal variations of the azimuthally averaged sound-speed structure in the upper two layers. In the upper layer, the averaged relative variation of the sound speed, $\delta c/c$, is $\sim -5 \times 10^{-4}$, the magnitude of which is somewhat higher than the variations of the surface temperature (Kuhn 1988), suggesting that the main changes occur beneath the photosphere, as was also noted by Kuhn (1988) and by Goode & Kuhn (1990). In the second layer, $\delta c/c \sim +6 \times 10^{-5}$.

The variations of the sound speed can be due to temperature change or due to magnetic field:

$$\frac{\delta c^2}{c^2} \approx \frac{\delta T}{T} + \frac{B^2}{8\pi p},$$

where p is the gas pressure. If the inferred variations are entirely due to magnetic field, then $\bar{B} \sim 5 \times 10^4$ G for the mean pressure in the second layer, $\bar{P} \sim 10^{11}$ dyn cm⁻² c⁻¹. This field strength is well above the low limit of 3×10^3 G established by Parker (1987).

It is interesting to note that the boundaries of the belt ($\approx \pm 10^\circ$) coincide with the most active latitude at the time of the observations (Solar-Geophysical Data 1991). There is also a hint for two narrow strips of reduced sound speed at latitude $\pm 22^\circ$, where active regions also emerged frequently.

The perturbations of the active regions can be seen in the two upper layers, but not deeper. The velocity maps (Fig. 3) show strong downflows of ≈ 1 km s⁻¹ around the sunspots, and some much weaker isolated upflows at the boundaries of the equatorial belt. The spatial resolution of the data is insufficient to study the structure and dynamics of individual sunspots. However, it is interesting to note that the peak of the downdraft velocity is observed between the spots in the bipolar group NOAA 6432 located at latitude -10° and longitude 20° . This group results in two separate strong negative sound-speed perturbations in the top layer (0–16 Mm), which merge into a single perturbation in the second layer (16–32 Mm). Figure 5 (Plate L10) (*top*) shows a vertical cut through this active region at a fixed latitude. The color map represents the sound-speed structure, and the arrows the projection of the velocity field into the longitude-depth plane. The convergent character of the flow is evident. This active region was only about 5 days old. The other young active regions in the observed area seem to show a similar pattern. In contrast, the much older decaying region NOAA 6427 (Fig. 5, *bottom*) shows reduced sound speed and diverging upflow. Another active region, NOAA 6437, with similar characteristics disappeared a day after it was observed. The flow patterns in the active regions seem to be consistent with the Doppler observations of the plasma motion on the solar surface (Gopasyuk 1967; Zwaan 1985).

In the flow maps (Fig. 3), the largest flow velocities are observed at the active latitudes $\pm 10^\circ$ and $\pm 22^\circ$. Some areas show strong flows without any apparent activity. At least, some of them could be the places where new magnetic structures emerged later—e.g., the area of strong converging flow seen in the two upper layers at latitude -8° and longitude 10° was close to the place where a new large group of sunspots, NOAA 6440, was born 2 days after.

4. DISCUSSION

Time-distance helioseismology pioneered by Duvall et al. (1993) gives us a three-dimensional look into the Sun's

interior, providing unique information about the structure and flows associated with magnetic field and turbulent convection. The interlink between convection and magnetic field results in the remarkable phenomenon of the solar cycle which has no analogy in the terrestrial laboratory.

In this Letter we have presented a technique and some initial results of inversion of the travel-time data which are sensitive to the sound-speed structure and to the flow velocity along sound-wave ray paths. A three-dimensional inversion method based on Fermat's principle and a regularized least-squares technique have been applied to infer the sound speed and the velocity of flows from the observations obtained at the South Pole on 1991 January 4–5 by Duvall et al. (1996). The spatial resolution of the inversion is $1^\circ 75$ in both longitude and latitude and 16 Mm in depth. The results for a four-layer model reveal large-scale subsurface sound-speed structures and flows related to the active regions.

We have found evidence for a large-scale low-latitude azimuthal structure which, possibly, can be associated with azimuthal magnetic flux bundles and a thermal shadow above them (Parker 1987) and, also, with thermal banding of solar convection (Brummell, Cattaneo, & Toomre, 1995). The magnetic flux bundles probably give rise to the magnetic Ω -loops emerging through the surface and observed as groups of sunspots (Parker 1994). However, the maximum amplitude of the azimuthal perturbation is found in the second layer, from 16 to 32 Mm, whereas, from theoretical arguments, the flux bundles should be concentrated near the bottom of the convection zone. The time-distance seismology has not yet reached that depth. Also, the current evidence is rather weak because of the large observational errors, but future travel-time data will certainly provide the information about the large-scale azimuthal structure, important for testing dynamo theories.

The emerging Ω -loops are expected to result in upwelling of the plasma in the active region. Instead, we see converging downflows in the places of recently emerged groups of sunspots and upwelling in decaying active regions, in agreement with the flow pattern observed on the solar surface. Also, there is evidence of different sound-speed structure in the developing and decaying regions. Obviously, continuous observations are necessary to study the dynamics of the active regions in detail.

Long-term tomographic monitoring of the solar convection zone using high-resolution data from the MDI experiment on *SOHO* (Scherrer et al. 1996) will provide a means for understanding the physics of solar convection and activity.

I thank Tom Duvall, Gene Parker, and Juri Toomre for useful discussions. This work was supported by a grant from NASA.

REFERENCES

- Brummell, N., Cattaneo, F., & Toomre, J. 1995, *Science*, 269, 1370
 Duvall, T. L., Jr., D'Silva, S., Jefferies, S. M., Harvey, J. W., & Schou, J. 1996, *Nature*, 379, 235
 Duvall, T. L., Jr., Jefferies, S. M., Harvey, J. W., & Pomerantz, M. A. 1993, *Nature*, 362, 430
 Goode, P. R., & Kuhn, J. R. 1990, *ApJ*, 356, 310
 Gopasyuk, S. I. 1967, *Izv. Krymsk. Astrofiz. Obs.*, 37, 29
 Howe, B. M., Worcester, P. F., & Spindel, R. C. 1987, *J. Geophys. Res.*, 92, 3785
 Iyer, H. M., & Hirahara, K., eds. 1993, *Seismic Tomography* (London: Chapman & Hall)
 Kuhn, J. R. 1988, *ApJ*, 331, L331
 Kuhn, J. R., Libbrecht, K. G., & Dicke, R. H. 1988, *Science*, 242, 908
 Paige, C. C., & Saunders, M. A. 1982, *ACM Trans. Math. Software*, 8, 43
 Parker, E. 1987, *ApJ*, 321, 984
 ———. 1994, *ApJ*, 433, 867
 Scherrer, P. H., et al. 1996, *Sol. Phys.*, 162, 129
 Zwaan, C. 1985, *Sol. Phys.*, 100, 397

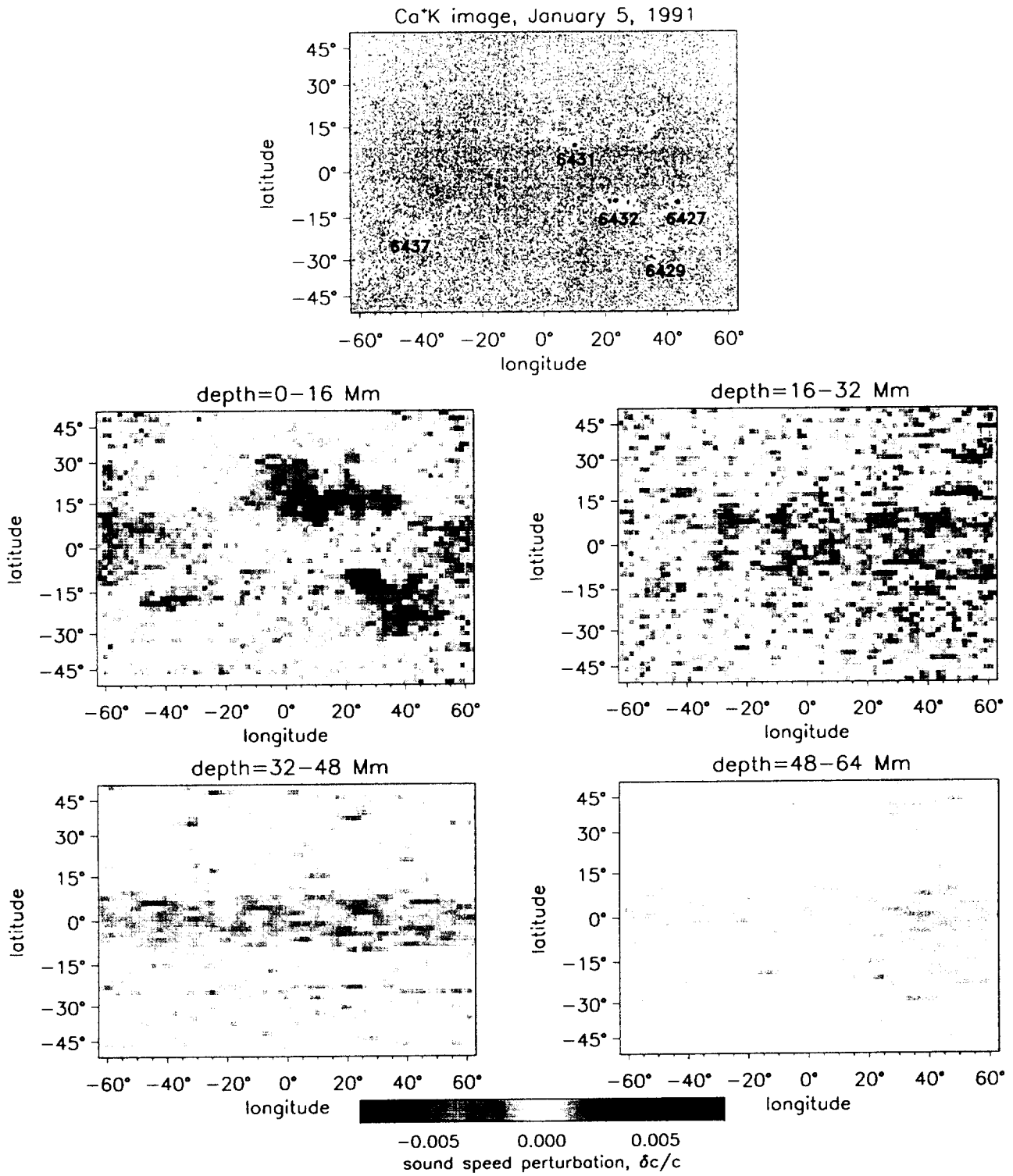


FIG. 2.—Ca⁺ K-line image of the observed area, and variations of the sound speed in the four-layer model of the upper convection zone relative to a horizontally uniform reference solar model.

KOSOVICH (see 461, L55)

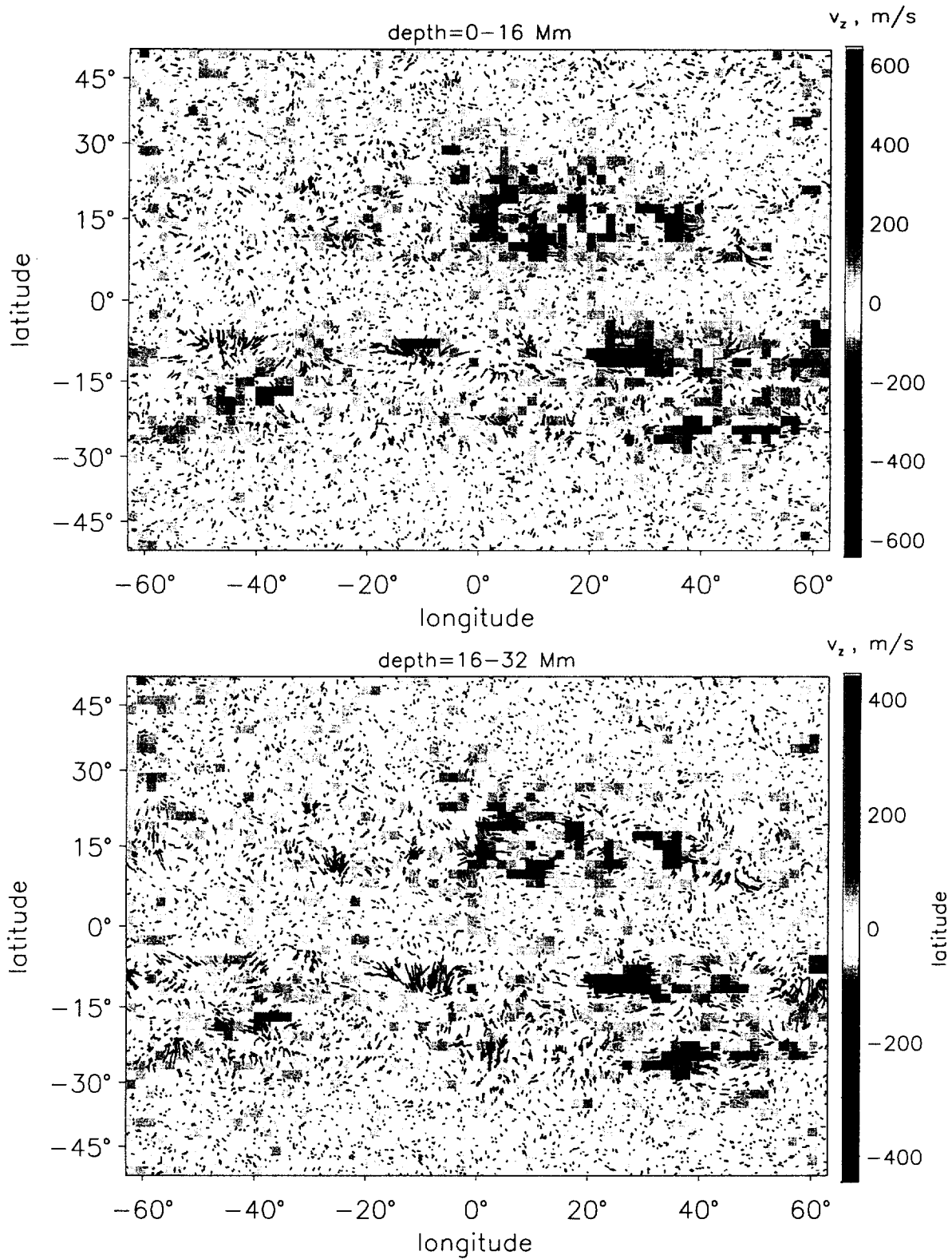


FIG. 3.—Vertical (color map) and horizontal (arrows) components of the flow velocity in the upper layer and in the second layer of the convection zone.

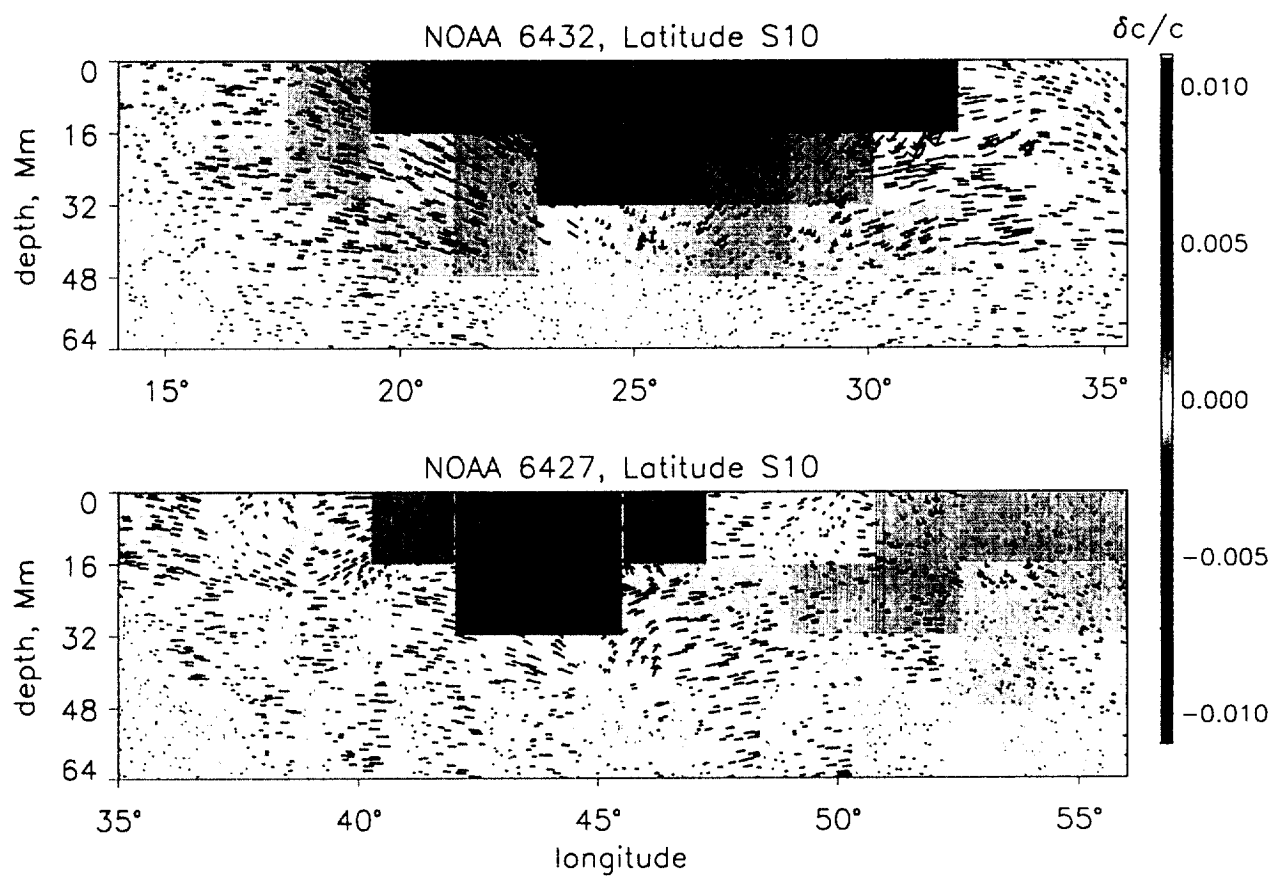


FIG. 5.—Variations of the sound speed (*color map*) and the flow velocity (*arrows*) as a function of depth and longitude at latitude -10° in growing active region NOAA 6432 (*top*), and in decaying region NOAA 6427 (*bottom*).

KOSOVICHEV (see 461, L57)

